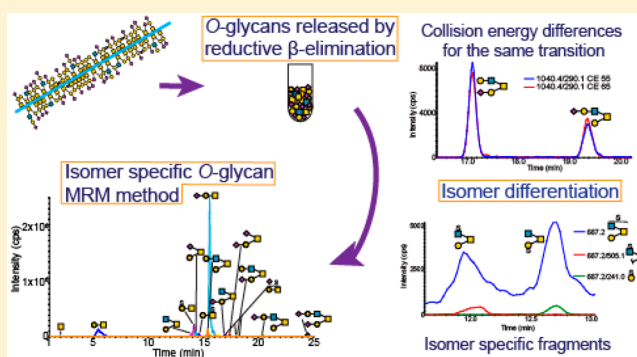


# Deciphering Isomers with a Multiple Reaction Monitoring Method for the Complete Detectable O-Glycan Repertoire of the Candidate Therapeutic, Lubricin

Sarah A. Flowers,<sup>\*,†,‡,§</sup> Catherine S. Lane,<sup>§</sup> and Niclas G. Karlsson<sup>†</sup><sup>†</sup>Department of Medical Biochemistry and Cell Biology, Institute of Biomedicine, Sahlgrenska Academy, University of Gothenburg, Medicinaregatan 9A, 40530 Gothenburg, Sweden<sup>‡</sup>Department of Neuroscience, Georgetown University, 3970 Reservoir Road NW, New Research Building EP20, Washington, D.C., United States<sup>§</sup>SCIEX, Phoenix House, Lakeside Drive, Centre Park, Warrington WA1 1RX, United Kingdom

## Supporting Information

**ABSTRACT:** Glycosylation is a fundamental post-translational modification, occurring on half of all proteins. Despite its significance, our understanding is limited, in part due to the inherent difficulty in studying these branched, multi-isomer structures. Accessible, detailed, and quantifiable methods for studying glycans, particularly O-glycans, are needed. Here we take a multiple reaction monitoring (MRM) approach to differentiate and relatively quantify all detectable glycans, including isomers, on the heavily O-glycosylated protein lubricin. Lubricin (proteoglycan 4) is essential for lubrication of the joint and eye. Given the therapeutic potential of lubricin, it is essential to understand its O-glycan repertoire in biological and recombinantly produced samples. O-Glycans were released by reductive  $\beta$ -elimination and defined, showing a range of 26 neutral, sulfated, sialylated, and both sulfated and sialylated core 1 (Gal $\beta$ 1-3GalNAc $\alpha$ 1-) and core 2 (Gal $\beta$ 1-3(GlcNAc $\beta$ 1-6)GalNAc $\alpha$ 1-) structures. Isomer-specific MRM transitions allowed effective differentiation of neutral glycan isomers as well as sulfated isomeric structures, where the sulfate was retained on the fragment ions. This strategy was not as effective with labile sialylated structures; instead, it was observed that the optimal collision energy for the  $m/z$  290.1 sialic acid B-fragment differed consistently between sialic acid isomers, allowing differentiation between isomers when fragmentation spectra were insufficient. This approach was also effective for purchased Neu5Ac $\alpha$ 2-3Gal $\beta$ 1-4Glc and Neu5Ac $\alpha$ 2-6Gal $\beta$ 1-4Glc and for Neu5Ac $\alpha$ 2-3Gal $\beta$ 1-4GlcNAc and Neu5Ac $\alpha$ 2-6Gal $\beta$ 1-4GlcNAc linkage isomers with the Neu5Ac $\alpha$ 2-6 consistently requiring more energy for optimal generation of the  $m/z$  290.1 fragment. Overall, this method provides an effective and easily accessible approach for the quantification and annotation of complex released O-glycan samples.



Our understanding of O-glycosylation in essential biological processes from lubrication<sup>1</sup> and defense<sup>2</sup> to interactions with other biomolecules in health and disease<sup>3</sup> continues to expand. O-Glycosylation alters in disease states such as cancers,<sup>4</sup> particularly of the gastrointestinal tract,<sup>5</sup> and chronic inflammation.<sup>6,7</sup> In these instances, we begin to see that specific structural changes may have biological implications: for instance, structural isomers differing between inflammation states in arthritic disease have been observed.<sup>7</sup> Annotation of O-glycan data is difficult, requiring practice and specialized skills and knowledge. The need to more accurately define the glycan structures on proteins of interest using a simpler methodology more accessible to a larger range of scientists is imperative to fully understand the meaning of these glycan changes in disease.

Lubricin is one such protein of interest, a heavily O-glycosylated mucin-like protein also known as superficial zone protein and proteoglycan 4, is found in the synovial fluid (SF) and joint tissues, where it is essential for boundary lubrication and protecting the cartilage surface.<sup>8–10</sup> Also found in the blood, urine, and ocular surface,<sup>11–13</sup> its 150 kDa backbone is doubled in mass by the 168 O-glycosylation sites identified primarily within the serine-, threonine-, and proline-rich central domain.<sup>14</sup> The lubricating properties of lubricin are conferred by its glycosylation, likely due to the high negatively charged sialic acid content it holds.<sup>15</sup> A recombinant form of the full-length lubricin protein, with a similar molecular mass,

Received: March 24, 2019

Accepted: June 27, 2019

Published: June 27, 2019

is an effective lubricant at the ocular surface<sup>12,16</sup> and may have potential for reforming the surface of the joint, lost during arthritis,<sup>17</sup> if administered at a very early stage of the disease. With this in mind, and given that a recombinant lubricin shows such promise as a biologic, it is important to be able to define and quantify the glycans on the native version to better understand the role of these glycans in health and disease.

GalNAc or mucin-type *O*-glycosylation biosynthesis begins with the addition of a GalNAc monosaccharide to the hydroxyl group of serine or threonine (Ser/Thr), referred to as Tn antigen (GalNAc $\alpha$ 1-), by one of 20 redundant uridine diphosphate-*N*-acetyl- $\alpha$ -D-galactosamine:polypeptide *N*-acetyl-galactosaminyltransferases (GalNAc transferases), which possess a range of unique and overlapping specificities.<sup>18</sup> The core 1 structure backbone (Gal $\beta$ 1-3GalNAc $\alpha$ 1-), formed by the addition of a galactose by core 1  $\beta$ 3-galactosyltransferase and the Cosmc chaperone,<sup>19</sup> can then go on to form the core 2 structure backbone (Gal $\beta$ 1-3(GlcNAc $\beta$ 1-6)GalNAc $\alpha$ 1-) by the core 2  $\beta$ -1,6-*N*-acetylglucosaminyltransferase family.<sup>20</sup> Lubricin, like the majority of *O*-glycosylated nonmucin proteins, holds both core 1 and 2 structures.<sup>21</sup> These core structures can then be extended by the addition of sialic acid, *N*-acetylneuraminic acid (Neu5Ac) in humans, by sialyltransferases<sup>22</sup> or sulfate by sulfotransferases,<sup>23</sup> giving an extensive range of isomeric structures.

Mass spectrometry is commonly agreed to be the most information rich method for analyzing glycans, although it is not without limitations and is aided by the power of separation techniques such as porous graphitized carbon liquid chromatography.<sup>24,25</sup> The intricacies of MS fragmentation complicate the understanding of the final data, particularly subtleties such as isomer differentiation, making annotation difficult. An *O*-glycan analytical method should reflect this subtlety while also being highly sensitive so that all isomers can be detected; here we describe an innovative MRM approach. Although this method is more difficult to develop in comparison to the data-dependent acquisition method most often used for *O*-glycan identification,<sup>24</sup> it is widely valued for stable quantification of both small and large molecules. MRM has also been applied to the field of glycobiochemistry, with the majority of work focusing on glycopeptides<sup>26–30</sup> and, to a lesser extent, released *N*-glycans.<sup>31,32</sup> The methods developed for *O*-glycans have been fewer<sup>33</sup> and more restricted, although they have shown biologically important results, such as focusing on subsets of biological- or disease-related *O*-glycans, including important sulfated *O*-glycans.<sup>7,34</sup> There have also been MRM analyses of oligosaccharides from human milk<sup>35,36</sup> as well as from bovine samples.<sup>37</sup> We take the novel approach of not only using MRM for quantification but also including additional transitions to allow the annotation of released *O*-glycans, including isomers. This greatly increases the ease of use to the end user, in effect building the *O*-glycan knowledge into the method, expanding accessibility. A QTRAP 6500 ESI-triple-quadrupole linear ion trap hybrid mass spectrometer<sup>38,39</sup> with its added ion trap functionality was able to facilitate method development for these challenging structures without standards. This meant that, although an extensive series of LC-MS optimization runs were necessary, the acquisition of full scan product ion spectra aided in fragment ion selection and a range of optimization and analysis, allowing extensive MRM method optimization without the infusion of standards.

## ■ EXPERIMENTAL SECTION

**Sample Preparation. Synovial Fluid Samples.** Pooled synovial lubricin samples were used for method development, given that more lubricin was required than is possible to obtain from a single patient and a consistent sample was required for comparison between a number of optimization runs. The pooled samples included samples from patients diagnosed with a range of arthritis diseases, both acute and chronic in nature, to cover the entire spectrum of potential glycans. Three pooled samples were prepared over the length of the study. Samples were grouped randomly into each of the pooled samples to obtain enough biological material for optimization of the MRM method for each single released *O*-glycan. The single sample that is shown in Figure 6 is from an individual who was diagnosed with rheumatoid arthritis and 36 years of age at collection. Synovial fluid (SF) samples were collected during aspiration of knee joints from arthritis patients at the Rheumatology Clinic, Sahlgrenska University Hospital (Gothenburg, Sweden). All patients fulfilled the American College of Rheumatology 1987 revised criteria for rheumatoid arthritis (RA).<sup>40</sup> All patients gave informed consent, and the procedure was approved by the Ethics Committee of University of Gothenburg. The SF samples were clarified by centrifugation at 10000g for 10 min and stored at  $-80$  °C until use.

**Preparation of Lubricin.** Lubricin was isolated via a multistage process. The acidic fraction was first isolated from SF samples by DEAE chromatography as previously described.<sup>41</sup> Briefly, SF samples were diluted with wash buffer (250 mM NaCl, 20 mM Tris-HCl, 10 mM EDTA, pH 7.5) and sheared with a needle and syringe before loading onto a 1 mL DEAE fast flow Hi-Trap column (GE Healthcare, Piscataway, NJ, USA). Enriched acidic glycoproteins were eluted with wash buffer containing 1.0 M NaCl. Eluted samples were concentrated and buffer-exchanged with PBS using Amicon Ultra 0.5 mL 30 kDa cutoff centrifugal filters (Millipore).

Samples were then reduced (50 mM DTT, 70 °C for 2 h) and alkylated (125 mM iodoacetamide for 30 min at room temperature in the dark) and separated by SDS-PAGE using NuPAGE 3–8% Tris-acetate gels (Thermo Fisher Scientific) to allow separation at the high molecular mass range. This cation exchange chromatography followed by SDS-PAGE has previously been shown by MS to effectively isolate lubricin.<sup>21</sup> Recombinant lubricin was also run on each gel as a positive control. The recombinant lubricin has previously been shown to have the same molecular mass as native lubricin when it is separated by SDS-PAGE.<sup>16</sup> Recombinant lubricin was a kind gift from Lubris BioPharma. Gels were transferred to a PVDF membrane by semidry transfer as previously described.<sup>42</sup> Membranes were stained with Alcian blue (0.125% Alcian blue in 25% methanol with 0.125% acetic acid) and destained with methanol.

**Standards.** Porcine gastric mucin (PGM) type II (Sigma M2378) was used for method optimization of glycans present on both PGM and lubricin. PGM *O*-glycans were released by reductive  $\beta$ -elimination, generating alditols for analysis. All structures and methods were confirmed with lubricin.

Glycan standards used to compare Neu5Ac linkage collision energy differences were obtained from Dextra Laboratories (Reading, U.K.). These included the Neu5Ac $\alpha$ 2-3Gal $\beta$ 1-4Glc (SL302) and Neu5Ac $\alpha$ 2-6Gal $\beta$ 1-4Glc (SL306), as well as the Neu5Ac $\alpha$ 2-3Gal $\beta$ 1-4GlcNAc (SLN302) and Neu5Ac $\alpha$ 2-6Gal $\beta$ 1-4GlcNAc (SLN306), isomer pairs. Glycans were

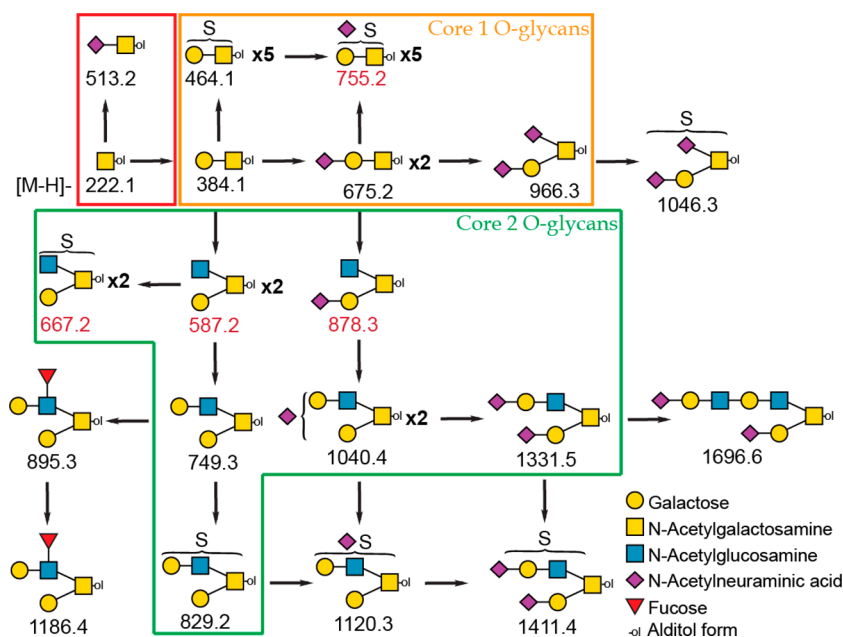


**Figure 1.** O-Glycan repertoire of lubricin. Core 1 O-glycans identified on lubricin are shown in the orange box, noncore simple structures in the red box, and predominately core 2 and larger glycans in the green box. The  $[M - H]^-$  value is shown under the structure diagram in black for previously identified structures and in red for structures not previously identified on lubricin. Structures outside the boxes were not identified on lubricin in the study but are monitored in the final method so that they can be evaluated should they be identified on future samples. An ambiguous structure or single structure is shown to represent isomers for simplicity. When one isomer is dominant as for the  $[M - H]^-$  values  $m/z$  675.2 and 587.2, the dominant isomer is shown. The number of isomers is shown in bold next to each structure ( $\times 2$ ,  $\times 5$ ). Arrows represent biosynthetic pathways.

solubilized in acetonitrile and water 20%/80% (v/v) with 10 mM ammonium bicarbonate at 5  $\mu\text{g}/\text{mL}$  and infused at 7  $\mu\text{L}/\text{min}$ . These standards were used without reduction.

**Release of O-Glycans.** The lubricin band was cut from the PVDF membrane and then into small pieces for O-glycan release. O-glycans were released by miniaturized reductive  $\beta$ -elimination,<sup>42</sup> allowing the sensitive release and detection of O-glycans including low-abundance sulfated and sialylated structures without interfering signals from introduced sample preparation contaminations. All glycans had a reducing end, making them alditols. O-Glycans from all arthritis samples were then pooled. Membrane pieces were placed in a 0.5 mL tube and wet with methanol before the addition of 20  $\mu\text{L}$  of freshly prepared reductive  $\beta$ -elimination solution (50 mM sodium hydroxide, 0.5 M sodium borohydride). The reactions were incubated at 50  $^\circ\text{C}$  for 16 h, in tubes that allowed gas exchange to the surrounding humidified environment. Glacial acetic acid (1  $\mu\text{L}$ ) was used to neutralize the reaction followed by cleanup. Cation exchange columns (AG50WX8 resin, Bio-Rad, Hercules, CA, USA) were prepared in 10  $\mu\text{L}$  pipet tips with 0.2  $\mu\text{L}$  of C18 resin held at the point of the tip (Ziptips; Millipore, Billerica, MA, USA). The C18 resin was used as a frit to hold the cation exchange resin and form a small column, and 40  $\mu\text{L}$  of cation exchange resin suspension (1:1 resin to methanol) was added to each tip column. Samples were added, and the released glycans that washed through the columns were collected, with residual glycans eluted with water. Samples were dried using a centrifugal evaporator (45  $^\circ\text{C}$ ) followed by extraction (five times) with 1% glacial acetic acid in methanol until all borate salts were removed. O-Glycans from all arthritis samples were then pooled, creating the sample used for method development. Glycans were released from the

PGM standard as described above, with the exception that the reductive  $\beta$ -elimination reaction was carried out in solution.

Glycans were released and detected as reduced alditols and it was assumed that all reducing ends were GalNAc-ol. O-glycans were identified by manual annotation of MS/MS spectra using previously described fragmentation principals.<sup>43</sup> Fragmentation patterns were also compared to the UniCarb-DB glycan MS/MS and retention time database<sup>44</sup> ([www.unicarb-db.org](http://www.unicarb-db.org)). Structures used accurately depict the level of annotation.

**LC and Mass Spectrometric Setup and Methodology.**  
**Liquid Chromatography.** Porous graphitized carbon (PGC) chromatography was used to separate isomers. PGC columns were 10 cm in length with an i.d. of 250  $\mu\text{m}$  and packed in house with 5  $\mu\text{m}$  particles (Hypercarb, Thermo). An Eksigent microLC 200 HPLC system (Eksigent, SCIEX, Redwood City, CA, USA) was used with a constant flow rate of 10  $\mu\text{L}/\text{min}$ . The gradient was as follows: 5 min of 98% solvent A (10 mM ammonium bicarbonate), increased solvent B (80% acetonitrile in 10 mM ammonium bicarbonate) from 2% to 45% in 41 min and then to 95% solvent B in 4 min, staying at 95% solvent B for 5 min, then re-equilibration at 98% A for 35 min.

**Mass Spectrometry.** The method was developed on a QTRAP 6500 triple-quadrupole linear ion trap mass spectrometer (SCIEX) in negative ion, high mass mode. A Turbo V ion source was used with an Eksigent 25  $\mu\text{m}$  electrode. An ion spray voltage of  $-4200$  V was used. MRM-specific voltages (collision energy, CE; declustering potential, DP; collision cell exit potential, CXP) were optimized for each transition (Table 1 in the Supporting Information). Each transition had a dwell time of 20 ms, which resulted in a cycle time sufficient to give 10 points on the curve to the fastest-eluting peak. All MRM transition selections and optimizations

were performed with an extensive series of LC-MS runs, because standards are not available for more efficient optimization by infusion. MRM fragment ion selection was facilitated by the use of the MIDAS workflow.<sup>45,46</sup> Using the MIDAS workflow, a set of MRM transitions was used as a survey scan to trigger the acquisition of highly sensitive linear ion trap MS/MS data. These data allowed confirmation of the glycan structure, isomer discrimination, and optimization of MRM fragment ion selection. MultiQuant 3.0 (SCIEX) was used for MRM peak integration. The method was run on two different QTRAP 6500 triple-quadrupole linear ion trap mass spectrometers (SCIEX) for comparison. MRM transition information and CXP (instrument dependent) information comparing instruments are given in Table 1 in the Supporting Information.

## RESULTS AND DISCUSSION

**Glycan Repertoire.** An MRM-initiated detection and sequencing approach was undertaken to scan for previously undetected glycans. The glycan repertoire of synovial lubricin was determined to consist of 26 glycan structures (Figure 1). Simple O-linked glycans were identified, at low abundance, including the Tn antigen (GalNAc) and sialyl Tn antigen (Neu5Ac $\alpha$ 2,6GalNAc). Twelve of the structures were core 1 structures (Gal $\beta$ 1-3GalNAcol), including structures with the addition of sulfate or Neu5Ac. Five isomers were also identified that held both a sulfate and Neu5Ac on the core 1 structure. A range of core 2 (Gal $\beta$ 1-3(GlcNAc $\beta$ 1-6)GalNAcol) structures were also identified, including structures with an additional galactose residue and/or Neu5Ac and sulfate. This direct approach at glycan discovery identified glycans not previously identified on lubricin, including structures with  $m/z$  755.2 (5 isomers, sulfated and sialylated trisaccharide), 667.2 (2 isomers, sulfated trisaccharide), 587.2 (2 isomers, neutral trisaccharide), and 878.3 (1 isomer, sialylated trisaccharide).<sup>21,47–49</sup> One sulfated and sialylated core 2 structure at  $m/z$  1120.3 was previously identified on lubricin isolated from a single osteoarthritis patient and was not identified in this study.<sup>21</sup>

**Neutral Glycans.** Five neutral structures were identified on lubricin (Figure 1) at  $[M - H]^-$   $m/z$  222.1, 384.1, and 749.3 and the two structures at  $m/z$  587.2. The GalNAcol monosaccharide structure was able to be retained on the PGC column. While this is usually difficult to isolate on PGC, it was possible using an extended re-equilibration, which increased the reproducibility of the retention of this monosaccharide. Although extending the LC method to almost 90 min, it gave the advantage of consistently re-equilibrating the PGC column to allow for monosaccharide retention, allowing the full coverage of the glycan repertoire with reproducible retention time. An MRM for the disaccharide, core 1 structure (Gal $\beta$ 1-3GalNAcol), has previously been described, including using cross-ring fragments that are rarely observed in other, larger glycans,<sup>7</sup> allowing for increased specificity. For the current method, the  $m/z$  204.1 Z fragment and  $m/z$  222.1 Y fragment showed the greatest intensity when the ion source and fragment parameters were optimized for intensity and stability (Figure 1 in the Supporting Information).

The  $[M - H]^-$  ion at  $m/z$  587.2 had two isomers, the branched (Gal $\beta$ 1-3(GlcNAc $\beta$ 1-6)GalNAcol) core 2 structure and a linear form (Figure 2). The linear form had a  $m/z$  407.17 Z<sub>1</sub> fragment, as shown in Figure 2, as well as the low-

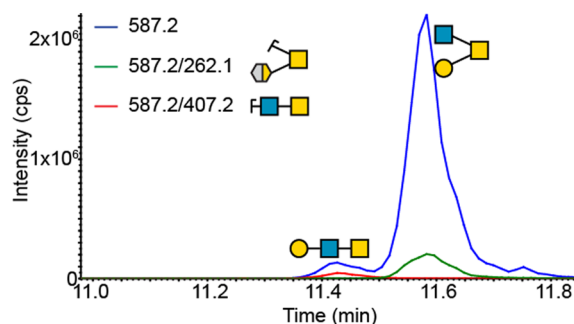


**Figure 2.** MRM identification of neutral glycans. Extracted ion chromatogram of two isomers from the PGM standard. The first eluting peak is shown by the  $m/z$  587.2/407.2 transition, which shows that the HexNAc and HexNAcol residues are adjoining. The second peak is shown by the  $m/z$  587.2/262.1 transition, the  ${}^4A_{0\alpha}$  fragment, identifying the core 2 branched structure.

abundance  $m/z$  425.17 Y<sub>1</sub> fragment, too low for effective MRM optimization and monitoring. These fragments indicate a HexNAc residue with an adjoining HexNAcol moiety, and the structure was confirmed to be the Gal $\beta$ 1-GlcNAc $\beta$ 1-3GalNAcol core 3 structure. The branched isomer included a prominent  $m/z$  262.1 ( ${}^4A_{0\alpha}$ ) fragment derived from the cleavage of the linear GalNAcol moiety. This peak was not observed in the linear form and has been shown to be indicative of the C-6 substitution of the GalNAcol moiety of core 2 structures.<sup>43</sup> The absence of this ion in the earlier eluting linear form is consistent with the fragmentation of previously identified Gal $\beta$ 1-GlcNAc $\beta$ 1-3GalNAcol.

The neutral glycan with  $[M - H]^-$  ion at  $m/z$  749.3 was identified as the branched core 2 glycan with the addition of a galactose residue and had only a single structure (Gal $\beta$ 1-3(Gal $\beta$ 1-4GlcNAc $\beta$ 1-6)GalNAcol). However, a larger range of transitions for annotation were included to exclude other potential structures, as well as to allow identification of additional potential isomers. For instance, a linear version of this composition is also possible (Gal $\beta$ 1-GlcNAc $\beta$ 1-Gal $\beta$ 1-3GalNAcol). As there are no adjacent HexNAc residues in this structure, it does not create the  $m/z$  407.17 fragment.<sup>2,43,50</sup> Hence, due to the separation ability of graphitized carbon, we would expect to find additional peaks with an  $[M - H]^-$  ion at  $m/z$  749.3, now without the  $m/z$  749.3/407.2 transition.

**Sulfated O-Glycans.** Three different sulfated glycan compositions were identified, including the compositions corresponding to sulfated core 1 ( $[M - H]^-$  ion at  $m/z$  464.1), sulfated core 2 trisaccharide ( $[M - H]^-$  ion at  $m/z$  667.2), and galactose extended core 2 tetrasaccharide. Only a single isomer of the  $[M - H]^-$  ion at  $m/z$  829.2 sulfated core 2 tetrasaccharide was identified, and transitions focused on the loss of galactose, including the Y-fragment transition  $m/z$  829.2/667.2.

The MRM differentiation of core 1 sulfated isomers has previously been described;<sup>7</sup> however, this study went on to further characterize these isomers. The retention of the sulfate on the monosaccharide unit makes isomer differentiation possible. The  $m/z$  corresponding to the sulfated core 1 presented up to five isomers in total; however, no single sample showed all of these isomers. Different batches of the pooled lubricin were shown to have different combinations of the three Gal-linked sulfate and two GalNAc-linked sulfate isomers (Figure 2 in the Supporting Information). This composition ( $[M - H]^-$  ion at  $m/z$  464.1) was the only one to show isomer

differences between batches, and the significance of the sulfated core 1 structure specifically to the inflammation state of the joint has been shown previously with alternate glycan profiles between chronic and acute disease states.<sup>7</sup> Given that the samples used in the pooled samples here were collected from patients as part of treatment, these are all from arthritis patients differing in specific disease diagnosis and stage. The presence of these five isomers indicates that traditional sulfate positions of 3- and 6-, on both Gal and GalNAc, cannot account for all of the identified isomers and nontraditional sites need to be considered. Sulfate migration has been observed previously,<sup>51</sup> apparent as a mixed isomer MS/MS in the same peak. Sulfate migration was not observed here using the QTRAP 6500 system, which would be observed as the identification of both the  $m/z$  464.1/241.0 and  $m/z$  464.1/302.1 transitions in the same peak.

The sulfated core 2 ( $[M - H]^-$  ion at  $m/z$  667.2), not previously identified on lubricin, was shown to have two isomers (Figure 3). Again, as sulfate was retained on intense

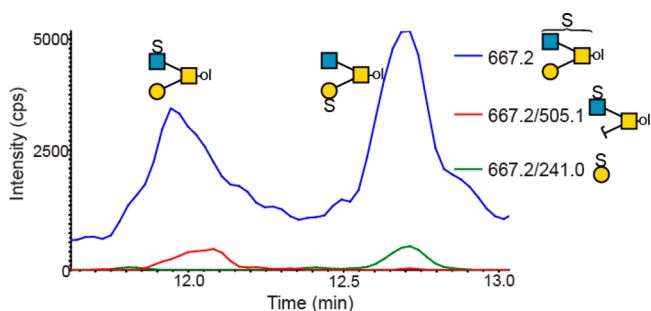


**Figure 3.** MRM identification of sulfated glycans. Extracted ion chromatograms of two isomers from a pooled lubricin sample. The first eluting peak at 12 min is shown by the  $m/z$  667.2/505.1 transition, the Y-type fragment (red), to have the sulfate attached at the GalNAc. The second peak is shown by the  $m/z$  667.2/241.0 transition, the B-type fragment (green), to hold the sulfate on the Gal residue.

fragments, MRM transitions were optimized for the  $m/z$  667.2/505.1 Y-type fragment as well as the  $m/z$  667.2/241.0 B-type fragment. This allowed the differentiation of the structures and annotation of the sulfate to the monosaccharide to which it was attached. The core 2 sulfation appears to be limited to Gal and GlcNAc residues.

**Sialylated O-Glycans.** Of the eight identified structures holding Neu5Ac, four structures including the sialylated GalNAc (sialyl Tn,  $[M - H]^-$  ion at  $m/z$  513.2), disialylated core 1 ( $[M - H]^-$  ion at  $m/z$  966.3), disialylated core 2 ( $[M - H]^-$  ion at  $m/z$  1331.5), and the low-abundance sialylated core 2 ( $[M - H]^-$  ion at  $m/z$  878.3) only displayed as single peaks in LC-MS, indicating single isomers. The presence of a single isomer was confirmed by fragmentation spectra. The optimized transitions for these structures focused primarily on quantification (Table 1 in the Supporting Information).

Sialic acid is labile; therefore, it is difficult to get consistent ions to differentiate isomers, since the one dominant peak is the prominent  $m/z$  290.1 Neu5Ac B fragment. Differentiation of the isomers was possible using an alternative MRM approach. The optimal CE for the same transition, using the Neu5Ac  $m/z$  290.1 fragment, was different between isomers. This allowed the same transition, at different CEs, to act as a differentiator between isomers. This also shows that CE not

only is a function of  $m/z$  or composition but also is directly affected by the structure of the glycan, apparent in multiple isomer pairs. The sialylated core 1 structure ( $[M - H]^-$  ion at  $m/z$  675.2) had two isomers, corresponding to branched (Gal $\beta$ 1,3(Neu5Ac $\alpha$ 2,6)GalNAcol) and linear (Neu5Ac $\alpha$ 2-3Gal $\beta$ 1-3GalNAcol) structures (Figure 4A). Differentiation

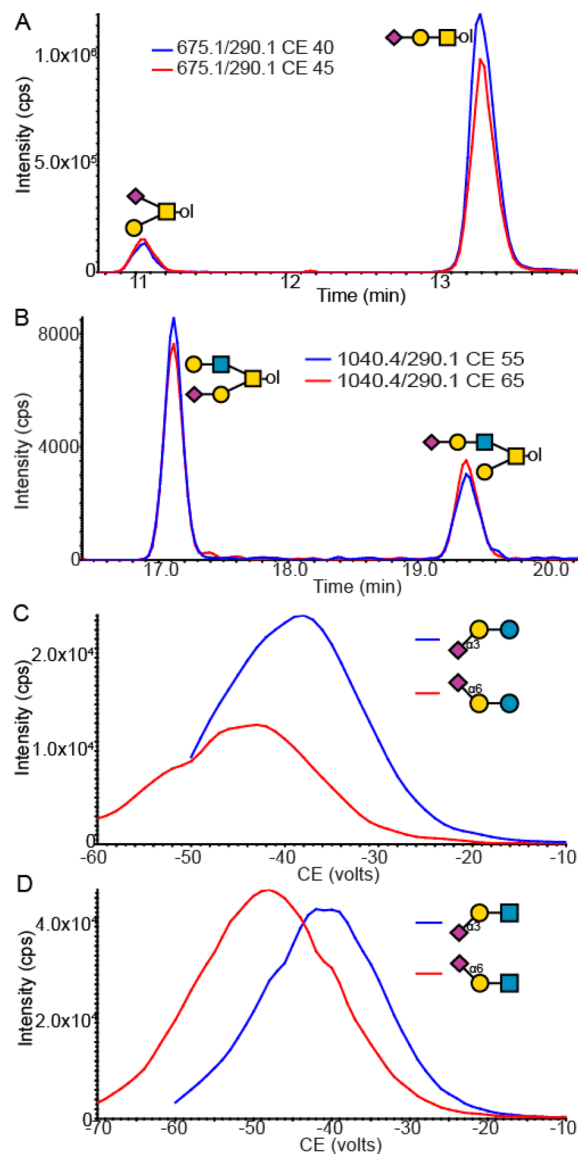


**Figure 4.** MRM identification of sialylated glycans by optimal CE. Extracted ion chromatogram of sialylated isomer pairs showing the same transition differing by CE. Isomer pairs are differentiated by the optimal CE for fragmentation of the Neu5Ac B fragment from the glycan structures. (A) MRM differentiation by optimal CE of Neu5Ac of sialylated core 1 branched and linear isomers from a pooled lubricin sample. (B) MRM differentiation by optimal CE of Neu5Ac position on core 2 pentasaccharide isomers from the pooled lubricin sample. (C) CE ramps of the  $m/z$  632.2/290.1 transition for the Neu5Ac $\alpha$ 2-3Gal $\beta$ 1-4Glc (blue) and Neu5Ac $\alpha$ 2-6Gal $\beta$ 1-4Glc (red) standards. (D) CE ramps of the  $m/z$  673.2/290.1 transition for the Neu5Ac $\alpha$ 2-3Gal $\beta$ 1-4GlcNAc (blue) and Neu5Ac $\alpha$ 2-6Gal $\beta$ 1-4GlcNAc (red) standards. Both CE ramps show a difference in the optimal CE for the release of Neu5Ac at  $m/z$  290.1, with the  $\alpha$ -2-3 linked Neu5Ac requiring less collision energy to release the peak amount of the  $m/z$  290.1 fragment in comparison to the  $\alpha$ -6 linked Neu5Ac.

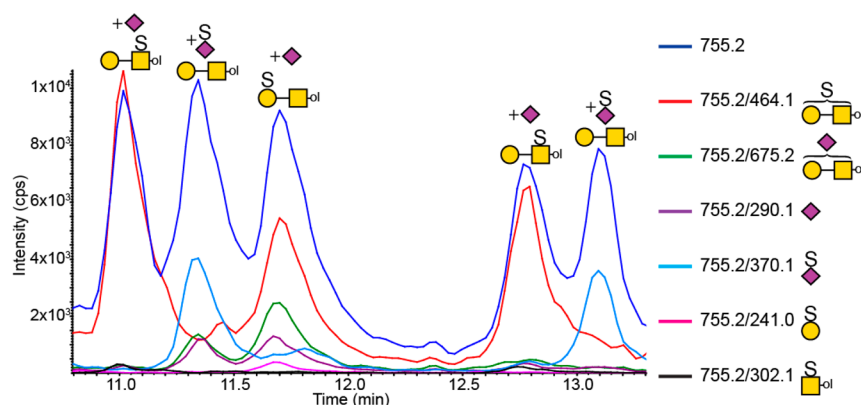


**Figure 5.** MRM identification of sulfated and sialylated core 1 glycans. Extracted ion chromatogram of five isomers from glycans released from a pooled lubricin sample separated by PGC chromatography. The parent is monitored in blue, showing all five isomers. The transitions to monitor sialylated fragments include  $m/z$  755.2/675.2 (core 1, green) and  $m/z$  755.2/290.1 (Neu5Ac, purple). The transitions to monitor sulfated fragments include  $m/z$  755.2/464.1 (core 1, red),  $m/z$  755.2/302.1 (GalNAc, black), and  $m/z$  755.2/241.0 (Gal, magenta). The  $m/z$  755.2/370.0 (aqua) transition is the sulfated Neu5Ac B-ion.

between the two isomers was made possible by use of the optimal CE for generation of the fragment at  $m/z$  290.1 fragment when *O*-glycans released from lubricin (Figure 4A), as well as from PGM (Figure 3 in the Supporting Information), were analyzed. This approach allowed the consistent differentiation of this isomer pair, where the diagnostic  $m/z$  495.2 Z fragment, which is also able to differentiate this pair, is very low in intensity and inconsistent even on optimization due to the labile nature of sialic acid on this small structure, as has been observed previously.<sup>52</sup> Another isomer pair, the monosialylated galactose extended core 2 structures ( $[M - H]^-$  ion at  $m/z$  1040.4), was annotated on the basis of PGC retention time with the Neu5Ac $\alpha$ 2-3Gal $\beta$ 1-3(Gal $\beta$ 1-4GlcNAc $\beta$ 1-6)GalNAc structure eluting before the Gal $\beta$ 1-3(Neu5Ac $\alpha$ 2-3Gal $\beta$ 1-4GlcNAc $\beta$ 1-6)GalNAc structure.<sup>53</sup> These isomers were also able to be differentiated by using a larger CE difference (CE 55 and 65, Figure 4B) in comparison to the core 1 structures ( $[M - H]^-$  ion at  $m/z$  675.2, CE 40 and 45, Figure 4A). The Neu5Ac $\alpha$ 2-3Gal $\beta$ 1-3(Gal $\beta$ 1-4GlcNAc $\beta$ 1-6)GalNAc structure had a lower optimal CE for the  $m/z$  1040.4/290.1 transition in comparison to the Gal $\beta$ 1-3(Neu5Ac $\alpha$ 2-3Gal $\beta$ 1-4GlcNAc $\beta$ 1-6)GalNAc structure. This showed that the CE difference is effective on a range of Neu5Ac isomer pairs, including linkage and position pairs.

Given that the optimal CE for Neu5Ac loss was different between isomers and hence able to differentiate isomeric pairs, standards were investigated to see if this approach would allow consistent differentiation between Neu5Ac $\alpha$ 2-3 and Neu5Ac $\alpha$ 2-6 linkage isomer pairs. Two isomer pairs were compared: Neu5Ac $\alpha$ 2-3Gal $\beta$ 1-4Glc and Neu5Ac $\alpha$ 2-6Gal $\beta$ 1-4Glc (Figure 4C) and Neu5Ac $\alpha$ 2-3Gal $\beta$ 1-4GlcNAc and Neu5Ac $\alpha$ 2-6Gal $\beta$ 1-4GlcNAc (Figure 4d). The optimal CE differed between the isomers in both of the isomer pairs. The optimal CE was also consistent between the pairs with the  $\alpha$ -2-6 linked isomer requiring additional energy to fragment the Neu5Ac from the glycan structure (Figure 4C,D). This agrees with previous reports that also showed more energy was required to remove the Neu5Ac, B fragment, from similar *O*-glycans and purchased standards.<sup>54,55</sup>

**Sulfated and Sialylated *O*-Glycans.** The addition of both a sulfate and Neu5Ac to the core 1 *O*-glycan ( $[M - H]^-$  ion at  $m/z$  755.2) gave a large range of isomeric structures, with five prominent isomers consistently observed on lubricin

(Figure 5). This makes annotation and differentiation difficult; however, it was able to be achieved using a range of transitions and PGC chromatography for isomer separation. This included transitions for sulfated fragments able to localize the sulfate either to the Gal or GalNAc (analyzed as the reduced GalNAcol) residue. These fragments were  $m/z$  241.0, the B fragment of the Gal-sulfated structure, and  $m/z$  302.1, the Y fragment of the GalNAc-sulfated structure. The sulfated core 1 fragment at  $m/z$  464.1 was also monitored. For Neu5Ac annotation the labile Neu5AcB fragment at  $m/z$  290.1 and the structure with loss of sulfate at  $m/z$  675.2 was monitored as well as the  $m/z$  370.0 fragment, which is the B fragment of a sulfated Neu5Ac residue. As discussed above, the labile nature of Neu5Ac, even when it is carefully optimized in negative ion mode, makes its location difficult to determine, particularly for lower abundance structures. The same was shown in the sulfated and sialylated structure, particularly when the sulfate was attached to the Neu5Ac residue. Despite these intricacies, this method was able to annotate and differentiate each of the five isomers. One isomer was Gal-sulfated (transition  $m/z$  755.2/241.0 observed, peak 3) and two GalNAc-sulfated (transition  $m/z$  755.2/302.1 observed, peaks 1 and 4), all with the addition of the Neu5Ac residue (transition  $m/z$  755.2/290.1 observed). The two others include the sulfated Neu5Ac (transition  $m/z$  755.2/370.0 observed, peaks 2 and 5). Neu5Ac can carry the sulfate at the hydroxyl groups of C-4, C-7, C-8, or C-9;<sup>56</sup> however, the location of the sulfate was unable to be determined in these analyses.

Little is known about the biological significance of the sulfated Neu5Ac, primarily due to the difficulty in analyzing this unstable structure. It has been detected in a limited range of biological samples, including sea urchin sperm and eggs.<sup>57,58</sup> Sulfated sialic acids have also been shown to have potentially critical pathogen and binding blocking roles, including in blocking HIV infection,<sup>59</sup> blocking of L- and P-selectin dependent cobra venom factor binding,<sup>60</sup> as well as inhibiting the cytotoxic effects of other snake venoms and bees<sup>61</sup> and inhibition of *in vitro* fertilization of mice,<sup>62</sup> although all of these studies have centered on low molecular mass sulfated Neu5Ac (2,8-linked Neu5Ac) polymers. The importance of the sulfated sialylated structures observed here on lubricin, a critical lubricating molecule of the human joint, is currently unknown and is of particular interest, given that the boundary

lubrication imparted by lubricin provides both a low binding and low friction surface to the joint.<sup>8–10</sup> It is essential to have subtle and sensitive methods, such as the method demonstrated here, to be able to continue such detailed *O*-glycan analyses to allow the comprehensive understanding of these poorly understood glycans.

**Final Method.** The final method included 77 transitions to differentiate and annotate the 26 structures as well as to monitor the parent mass (singly and doubly charged) of six other larger structures (Figure 1), the next likely extensions as apparent from other mucin proteins.<sup>6,50</sup> Should these be identified, then that patient sample can be used to optimize more specific transitions for the identified structures and extend the MRM method. This is important, because it was essential to optimize conditions such as CE specifically for each isomer, and therefore samples with the necessary isomer profile are required for MRM optimization.

This method allows the full definition of the glycan structures described here, and although separation with the PGC chromatography is ideal, particularly for sialylated isomers, the method does not rely on the chromatographic pattern to define isomers. This is essential given that an isomer may be missing, as observed with the sulfated core 1 structures.

The MRM approach is sensitive: low-abundance intermediary structures were able to be identified and quantified that have not previously been identified on lubricin. These low-abundance structures included the  $[M - H]^-$  ion at  $m/z$  587.2 corresponding to the core 2 structure and the  $[M - H]^-$  ion at  $m/z$  755.2 corresponding to the sulfated and sialylated core 1 structures. It is also able to identify these structures using a single patient sample, as shown in Figure 6, which shows the *O*-glycans released from lubricin isolated from an RA patient. Core 1 structures, unmodified, and the linear sialylated

structure (Neu5Ac $\alpha$ 2-3Gal $\beta$ 1-3GalNAc $\alpha$ 1), dominate the glycoprofile of lubricin, with other core 1 and core 2 structures of a much lower intensity (Figure 6). This glycoprofile is similar to what has been described previously for lubricin;<sup>14,21</sup> however, this MRM method had the addition of the identification of the previously undetected low-abundance glycans.

## CONCLUSIONS

Different glycan classes are best annotated by specific MRM approaches. Neutral monosaccharides and sulfate are retained during optimized fragmentation, allowing annotation through isomer-specific transitions. Sialic acid is more labile, but the loss of the Neu5Ac  $m/z$  290.1 fragment B-ion is optimal at different CE for different Neu5Ac-containing isomers. The generation of this fragment is also characteristic, following consistent trends of structure and linkage such as an increased collision energy required for the  $\alpha$ 2-6 linked Neu5Ac in comparison to the  $\alpha$ 2-3 linked Neu5Ac. This approach allows identification and annotation of the structure in a manner that is simplified with the presence of specific peaks or relative abundance of the same transition at different CEs.

The sensitivity of this approach allowed the identification of a range of novel *O*-glycan structures, including five isomers of the sulfated and sialylated core 1 structure, two of which contained a sulfated sialic acid. Five isomers of the sulfated core 1 structure were also identified, three Gal-linked and two GalNAc-linked.

The inclusion of a broader range of larger glycans, not yet identified on lubricin, allows for the potential identification of these glycans in future samples, giving the method flexibility. Taking a novel approach to the MRM method rather than focusing only on data analysis opens up this flexibility.

Annotation of *O*-glycans is difficult, requiring practice and specialized skills and knowledge. Creating an isomer-specific MRM profile for each structure, as shown here, makes the method accessible to a broader audience because the profiles have already been defined. This method is also suitable for routine automation and high-throughput analyses of released *O*-glycan samples.

## ASSOCIATED CONTENT

### Supporting Information

The Supporting Information is available free of charge on the ACS Publications website at DOI: 10.1021/acs.analchem.9b01485.

Parameters for MRM transitions, fragmentation spectra for core 1 *O*-glycans, MRM differentiation of sulfated core 1 structures from different pooled lubricin samples, and MRM differentiation of sialylated core 1 structures from porcine gastric mucin (PDF)

## AUTHOR INFORMATION

### Corresponding Author

\*E-mail for S.A.F.: saf76@georgetown.edu.

### ORCID

Sarah A. Flowers: 0000-0002-3513-2260

### Notes

The authors declare the following competing financial interest(s): The authors declare no competing financial interest. SCIEX provided no financial support for the work

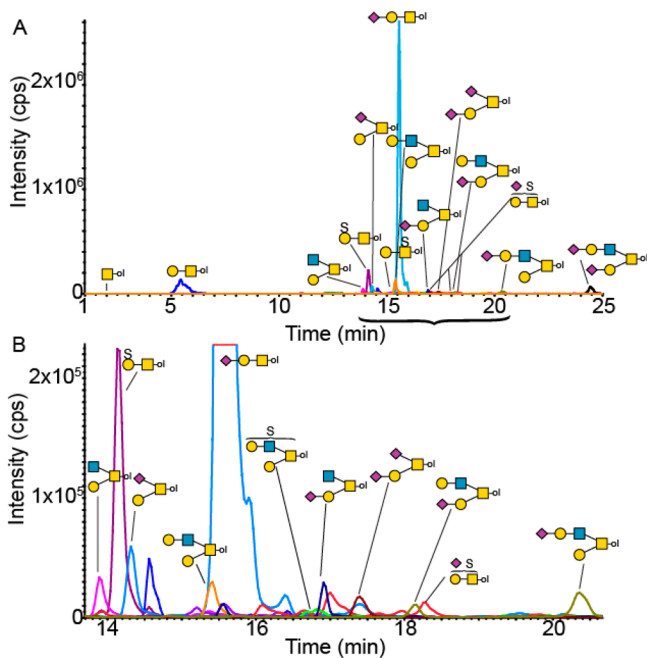


**Figure 6.** MRM identification of all released glycans from lubricin isolated from a patient's SF. (A) Extracted ion chromatogram of all released glycans from a single patient's lubricin sample separated by PGC chromatography. Each glycan is shown by a single MRM transition for simplicity. (B) Closeup of lower abundance glycans from panel A.

undertaken or final say in the decision to publish or the content of the publication.

## ACKNOWLEDGMENTS

S.A.F. and N.G.K. acknowledge funding from grants for the Swedish state under the agreement between the Swedish government and the county council, the ALF-agreement (ALFGBG-722391), The Swedish Foundation for International Cooperation in Research and Higher Education (STINT), the Swedish Research Council (621-2013-5895), Kung Gustav V:s 80-Års foundation, Petrus and Augusta Hedlund's foundation (M-2016-0353), and AFA insurance research fund (dnr 150150). The authors thank Dr. Lena Björkman at Sahlgrenska University Hospital for supplying synovial fluid samples. We also thank Lubris BioPharma for the recombinant lubricin used as a lubricin standard for gel separation.

## REFERENCES

- (1) Coles, J. M.; Chang, D. P.; Zauscher, S. *Curr. Opin. Colloid Interface Sci.* **2010**, *15*, 406–416.
- (2) Everest-Dass, A. V.; Jin, D.; Thaysen-Andersen, M.; Nevalainen, H.; Kolarich, D.; Packer, N. H. *Glycobiology* **2012**, *22*, 1465–1479.
- (3) Cohen, M. *Biomolecules* **2015**, *5*, 2056–2072.
- (4) Kudelka, M. R.; Ju, T.; Heimbürg-Molinari, J.; Cummings, R. D. *Adv. Cancer Res.* **2015**, *126*, 53–135.
- (5) Ferreira, J. A.; Magalhaes, A.; Gomes, J.; Peixoto, A.; Gaiteiro, C.; Fernandes, E.; Santos, L. L.; Reis, C. A. *Cancer Lett.* **2017**, *387*, 32.
- (6) Chaudhury, N. M.; Proctor, G. B.; Karlsson, N. G.; Carpenter, G. H.; Flowers, S. A. *Mol. Cell. Proteomics* **2016**, *15*, 1048–1059.
- (7) Flowers, S. A.; Ali, L.; Lane, C. S.; Olin, M.; Karlsson, N. G. *Mol. Cell. Proteomics* **2013**, *12*, 921–931.
- (8) Gleghorn, J. P.; Bonassar, L. J. *J. Biomech.* **2008**, *41*, 1910–1918.
- (9) Jones, A. R.; Gleghorn, J. P.; Hughes, C. E.; Fitz, L. J.; Zollner, R.; Wainwright, S. D.; Caterson, B.; Morris, E. A.; Bonassar, L. J.; Flannery, C. R. *J. Orthop. Res.* **2007**, *25*, 283–292.
- (10) Nugent-Derfus, G. E.; Chan, A. H.; Schumacher, B. L.; Sah, R. L. *J. Orthop. Res.* **2007**, *25*, 1269–1276.
- (11) Liu, Y. J.; Lu, S. H.; Xu, B.; Yang, R. C.; Ren, Q.; Liu, B.; Li, B.; Lu, M.; Yan, F. Y.; Han, Z. B.; Han, Z. C. *Blood* **2004**, *103*, 4449–4456.
- (12) Schmidt, T. A.; Sullivan, D. A.; Knop, E.; Richards, S. M.; Knop, N.; Liu, S.; Sahin, A.; Darabad, R. R.; Morrison, S.; Kam, W. R.; Sullivan, B. D. *JAMA ophthalmology* **2013**, *131*, 766–776.
- (13) Su, J. L.; Schumacher, B. L.; Lindley, K. M.; Soloveyichik, V.; Burkhart, W.; Triantafillou, J. A.; Kuettner, K.; Schmid, T. *Hybridoma* **2001**, *20*, 149–157.
- (14) Ali, L.; Flowers, S. A.; Jin, C.; Bennet, E. P.; Ekwall, A. K.; Karlsson, N. G. *Mol. Cell. Proteomics* **2014**, *13*, 3396–3409.
- (15) Jay, G. D.; Harris, D. A.; Cha, C. J. *Glycoconjugate J.* **2001**, *18*, 807–815.
- (16) Samsom, M. L.; Morrison, S.; Masala, N.; Sullivan, B. D.; Sullivan, D. A.; Sheardown, H.; Schmidt, T. A. *Exp. Eye Res.* **2014**, *127*, 14–19.
- (17) Vugmeyster, Y.; Wang, Q.; Xu, X.; Harrold, J.; Daugusta, D.; Li, J.; Zollner, R.; Flannery, C. R.; Rivera-Bermudez, M. A. *AAPS J.* **2012**, *14*, 97–104.
- (18) Brockhausen, I.; Schachter, H.; Stanley, P. In *Essentials of Glycobiology*; Varki, A., Cummings, R. D., Esko, J. D., Freeze, H. H., Stanley, P., Bertozzi, C. R., Hart, G. W., Etzler, M. E., Eds.; Cold Spring Harbor Press: 2009.
- (19) Ju, T.; Cummings, R. D. *Proc. Natl. Acad. Sci. U. S. A.* **2002**, *99*, 16613–16618.
- (20) Schwientek, T.; Nomoto, M.; Levery, S. B.; Merckx, G.; van Kessel, A. G.; Bennett, E. P.; Hollingsworth, M. A.; Clausen, H. *J. Biol. Chem.* **1999**, *274*, 4504–4512.
- (21) Estrella, R. P.; Whitelock, J. M.; Packer, N. H.; Karlsson, N. G. *Biochem. J.* **2010**, *429*, 359–367.
- (22) Patel, R. Y.; Balaji, P. V. *Glycobiology* **2006**, *16*, 108–116.
- (23) Brockhausen, I. *Biochem. Soc. Trans.* **2003**, *31*, 318–325.
- (24) Mulagapati, S.; Koppolu, V.; Raju, T. S. *Biochemistry* **2017**, *56*, 1218–1226.
- (25) Stavenhagen, K.; Kolarich, D.; Wuhler, M. *Chromatographia* **2015**, *78*, 307–320.
- (26) Shah, A. K.; Cao, K. A.; Choi, E.; Chen, D.; Gautier, B.; Nancarrow, D.; Whiteman, D. C.; Saunders, N. A.; Barbour, A. P.; Joshi, V.; Hill, M. M. *Mol. Cell. Proteomics* **2015**, *14*, 3023–3039.
- (27) Hong, Q.; Lebrilla, C. B.; Miyamoto, S.; Ruhaak, L. R. *Anal. Chem.* **2013**, *85*, 8585–8593.
- (28) Ahn, Y. H.; Lee, J. Y.; Lee, J. Y.; Kim, Y. S.; Ko, J. H.; Yoo, J. S. *J. Proteome Res.* **2009**, *8*, 4216–4224.
- (29) Zhao, Y.; Jia, W.; Wang, J.; Ying, W.; Zhang, Y.; Qian, X. *Anal. Chem.* **2011**, *83*, 8802–8809.
- (30) Huang, J.; Kailemia, M. J.; Goonatilke, E.; Parker, E. A.; Hong, Q.; Sabia, R.; Smilowitz, J. T.; German, J. B.; Lebrilla, C. B. *Anal. Bioanal. Chem.* **2017**, *409*, 589–606.
- (31) Zhang, H.; Wang, Z.; Stupak, J.; Ghribi, O.; Geiger, J. D.; Liu, Q. Y.; Li, J. *Proteomics* **2012**, *12*, 2510–2522.
- (32) Zhou, S.; Wooding, K. M.; Mechref, Y. *Methods Mol. Biol.* **2017**, *1503*, 83–96.
- (33) Darula, Z.; Medzihradzky, K. F. *Mol. Cell. Proteomics* **2018**, *17*, 2–17.
- (34) Tanaka-Okamoto, M.; Mukai, M.; Takahashi, H.; Fujiwara, Y.; Ohue, M.; Miyamoto, Y. *Glycobiology* **2016**, *27*, 400–415.
- (35) Xu, G.; Davis, J. C.; Goonatilke, E.; Smilowitz, J. T.; German, J. B.; Lebrilla, C. B. *J. Nutr.* **2017**, *147*, 117–124.
- (36) Mank, M.; Welsch, P.; Heck, A. J. R.; Stahl, B. *Anal. Bioanal. Chem.* **2019**, *411*, 231–250.
- (37) Fong, B.; Ma, K.; McJarrow, P. *J. Agric. Food Chem.* **2011**, *59*, 9788–9795.
- (38) Hager, J. W.; Yves Le Blanc, J. C. *Rapid Commun. Mass Spectrom.* **2003**, *17*, 1056–1064.
- (39) Le Blanc, J. C.; Hager, J. W.; Ilisiu, A. M.; Hunter, C.; Zhong, F.; Chu, I. *Proteomics* **2003**, *3*, 859–869.
- (40) Arnett, F. C.; Edworthy, S. M.; Bloch, D. A.; McShane, D. J.; Fries, J. F.; Cooper, N. S.; Healey, L. A.; Kaplan, S. R.; Liang, M. H.; Luthra, H. S.; et al. *Arthritis Rheum.* **1988**, *31*, 315–324.
- (41) Estrella, R. P.; Whitelock, J. M.; Packer, N. H.; Karlsson, N. G. *Biochem. J.* **2010**, *429*, 359–367.
- (42) Hayes, C. A.; Nemes, S.; Issa, S.; Jin, C.; Karlsson, N. G. *Methods Mol. Biol.* **2012**, *842*, 141–163.
- (43) Karlsson, N. G.; Schulz, B. L.; Packer, N. H. *J. Am. Soc. Mass Spectrom.* **2004**, *15*, 659–672.
- (44) Hayes, C. A.; Karlsson, N. G.; Struwe, W. B.; Lisacek, F.; Rudd, P. M.; Packer, N. H.; Campbell, M. P. *Bioinformatics* **2011**, *27*, 1343–1344.
- (45) Unwin, R. D.; Griffiths, J. R.; Leverentz, M. K.; Grallert, A.; Hagan, I. M.; Whetton, A. D. *Mol. Cell. Proteomics* **2005**, *4*, 1134–1144.
- (46) Cox, D. M.; Zhong, F.; Du, M.; Duchoslav, E.; Sakuma, T.; McDermott, J. C. *J. Biomol. Tech.* **2005**, *16*, 83–90.
- (47) Jin, C.; Ekwall, A. K.; Bylund, J.; Bjorkman, L.; Estrella, R. P.; Whitelock, J. M.; Eisler, T.; Bokarewa, M.; Karlsson, N. G. *J. Biol. Chem.* **2012**, *287*, 35922–35933.
- (48) Ali, L.; Kenny, D. T.; Hayes, C. A.; Karlsson, N. G. *Metabolites* **2012**, *2*, 648–666.
- (49) Ali, L.; Flowers, S. A.; Jin, C.; Bennet, E. P.; Ekwall, A. K.; Karlsson, N. G. *Mol. Cell. Proteomics* **2014**, *13*, 3396–3409.
- (50) Karlsson, N. G.; Thomsson, K. A. *Glycobiology* **2009**, *19*, 288–300.
- (51) Kenny, D. T.; Issa, S.; Karlsson, N. G. *Rapid Commun. Mass Spectrom.* **2011**, *25*, 2611–2618.
- (52) Everest-Dass, A. V.; Abrahams, J. L.; Kolarich, D.; Packer, N. H.; Campbell, M. P. *J. Am. Soc. Mass Spectrom.* **2013**, *24*, 895–906.



- (53) Liu, J.; Jin, C.; Cherian, R. M.; Karlsson, N. G.; Holgersson, J. J. *Biotechnol.* **2015**, *199*, 77–89.
- (54) Seymour, J. L.; Costello, C. E.; Zaia, J. *J. Am. Soc. Mass Spectrom.* **2006**, *17*, 844–854.
- (55) Chen, C.; Lin, Y.; Lin, J.; Li, S.; Ren, C.; Wu, C.; chen, C. *Isr. J. Chem.* **2015**, *55*, 412–422.
- (56) Varki, A.; Schnaar, R. L.; Schauer, R.; Varki, A.; Cummings, R. D.; Esko, J. D.; Stanley, P.; Hart, G. W.; Aebi, M.; Darvill, A. G.; Kinoshita, T.; Packer, N. H.; Prestegard, J. H.; Schnaar, R. L.; Seeberger, P. H. *Essentials of Glycobiology*; Cold Spring Harbor: 2015; pp 179–195.
- (57) Yamakawa, N.; Sato, C.; Miyata, S.; Maehashi, E.; Toriyama, M.; Sato, N.; Furuhashi, K.; Kitajima, K. *Biochimie* **2007**, *89*, 1396–1408.
- (58) Miyata, S.; Sato, C.; Kitamura, S.; Toriyama, M.; Kitajima, K. *Glycobiology* **2004**, *14*, 827–840.
- (59) Clayton, R.; Hardman, J.; LaBranche, C. C.; McReynolds, K. D. *Bioconjugate Chem.* **2011**, *22*, 2186–2197.
- (60) Mulligan, M. S.; Warner, R. L.; Lowe, J. B.; Smith, P. L.; Suzuki, Y.; Miyasaka, M.; Yamaguchi, S.; Ohta, Y.; Tsukada, Y.; Kiso, M.; Hasegawa, A.; Ward, P. A. *International immunology* **1998**, *10*, 569–575.
- (61) Oda, Y.; Kinoshita, M.; Hamada, K.; Nakayama, K.; Ohta, Y.; Yamaguchi, S.; Tsukada, Y.; Kawai, Y.; Kakehi, K. *Glycoconjugate J.* **1999**, *16*, 457–463.
- (62) Kawai, Y.; Takemoto, M.; Oda, Y.; Kakehi, K.; Ohta, Y.; Yamaguchi, S.; Miyake, M. *Biol. Pharm. Bull.* **2000**, *23*, 936–940.